

ELECTRONIC SUPPLEMENTARY INFORMATION

Explanation and screen shots of data processing software

Python-based data processing software for MS Windows (<https://github.com/metarapi/Laser-Ablation-Simulation-Tool/releases/latest>) was developed to simulate the process of LA-ICP-TOFMS mapping of elements in soft biological tissues, focusing on the visualization of the experimental element-specific SPR profiles (T. Van Helden et al., Anal. Chim. Acta 1287 (2024) 342089), and their impact on image quality under various selectable virtual mapping conditions (dosage, lateral scan speed, repetition rate, Flicker noise, and concentration). The application highlights the effects of image smear and noise induced by the SPR profiles on a phantom image (Johannes Vermeer, “Girl with a Pearl Earring”, ca. 1665). Built with Python, the application leverages customtkinter for an interactive user interface and matplotlib for comprehensive plotting capabilities.

The application contains two functionalities, selectable via option buttons:

SPR Profiles

Visualization of the experimental element-specific SPR profiles for 22 nuclides [i] at 30 fluences [F] ranging from 0.07 to 6.3 J cm⁻², selectable via an option button and slider, respectively. Each SPR profile is based on an average of 100 single laser shots on a gelatinous droplet standard (serving as a proxy for soft biological tissue), spiked with a multi-element standard to a concentration [$C_{gel}(i)$] of 100 µg g⁻¹, using a 20 µm diameter circular laser beam [BS] at the chosen fluence.

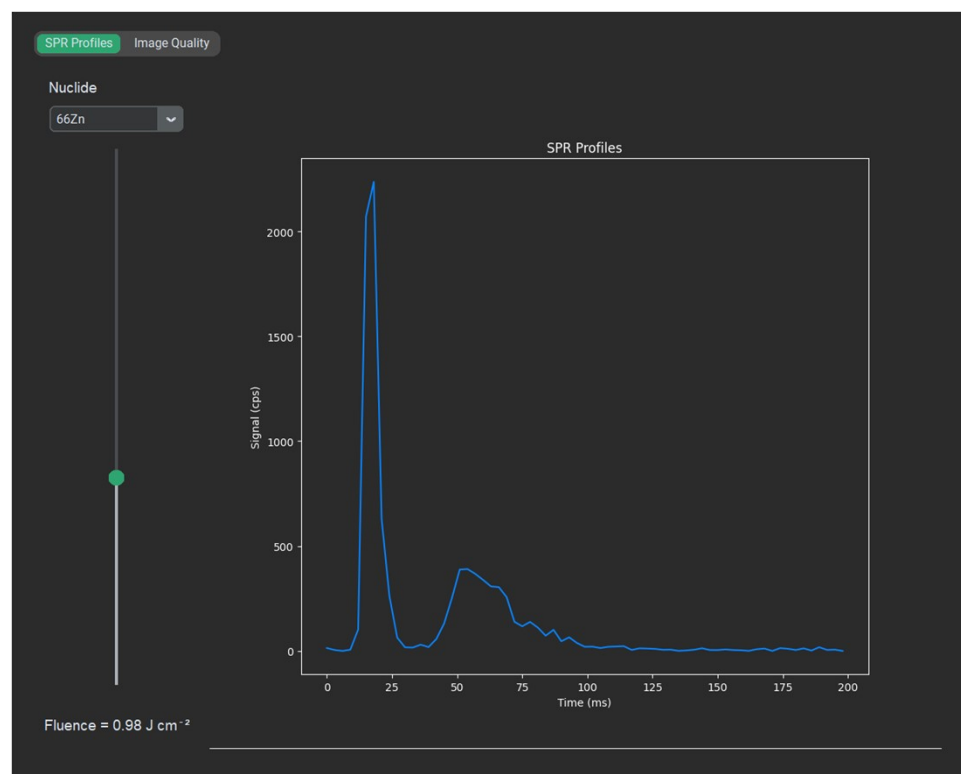


Fig S1. Experimental element-specific SPR profiles for different nuclides at selected fluences.

Image Quality

Image degradation is modeled for an 8-bit phantom ($3,000 \times 3,000$ square pixels, each pixel measuring $1 \mu\text{m} \times 1 \mu\text{m}$) upon virtual LA-ICP-TOFMS mapping. The phantom is treated as a “gelatinous sample” and mapped with the same circular laser beam [BS] and fluence [F] used for recording the SPR profiles described above. We assume that the phantom and gelatinous droplet standard share the same ablation characteristics.

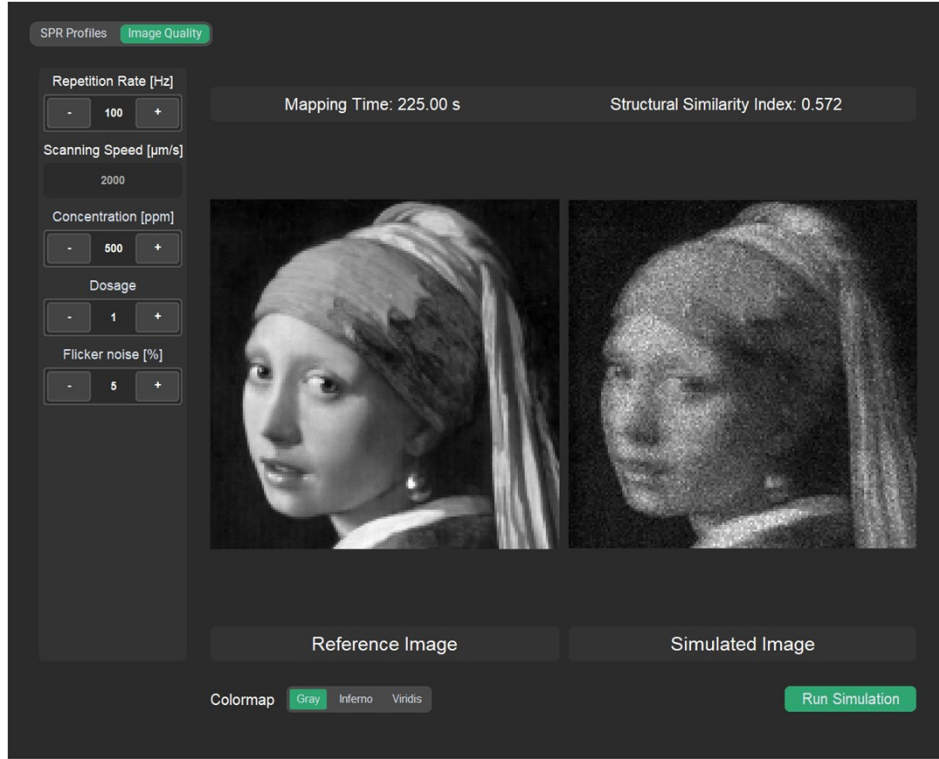


Fig S2. Reference image (phantom) and degraded image after virtual LA-ICP-TOFMS mapping with user-selected mapping conditions. Mapping time and SSIM index are an indication of pixel acquisition rate and image quality.

Mapping parameters that can be adjusted by the user through scrolling with the mouse wheel (for large steps) or the + and - buttons (for small steps) include the repetition rate [$1 \leq RR \leq 1,000$ Hz], maximum concentration in the phantom [$1 \leq C_{\text{phant}}(i) \leq 10,000 \mu\text{g g}^{-1}$], dosage [$D = 1, 2, 5, 10, \text{ or } 20$], and flicker noise [$1 \leq SD_f \leq 20$ %]. The lateral scan speed [SS] is inferred and calculated from the repetition rate and the dosage using $SS = (BS \cdot RR)/D$. To select a specific lateral scan speed, one needs to adjust the repetition rate and/or dosage (with the beam size fixed at $20 \mu\text{m}$), while the mapping time is calculated to assess the pixel acquisition rate's impact on image quality. The impact of the selected mapping conditions on the image quality of the virtually mapped phantom can be observed by running the simulation and comparing the reference image with the simulated image, color-mapped in Gray, Inferno, or Viridis. Objective evaluation is possible through the Structural Similarity Index (SSIM), providing a quantitative measure of image quality degradation ($0 \leq \text{SSIM} \leq 1$; a value of 1 indicates a perfect match).

Experimental demonstration of element-dependent image degradation

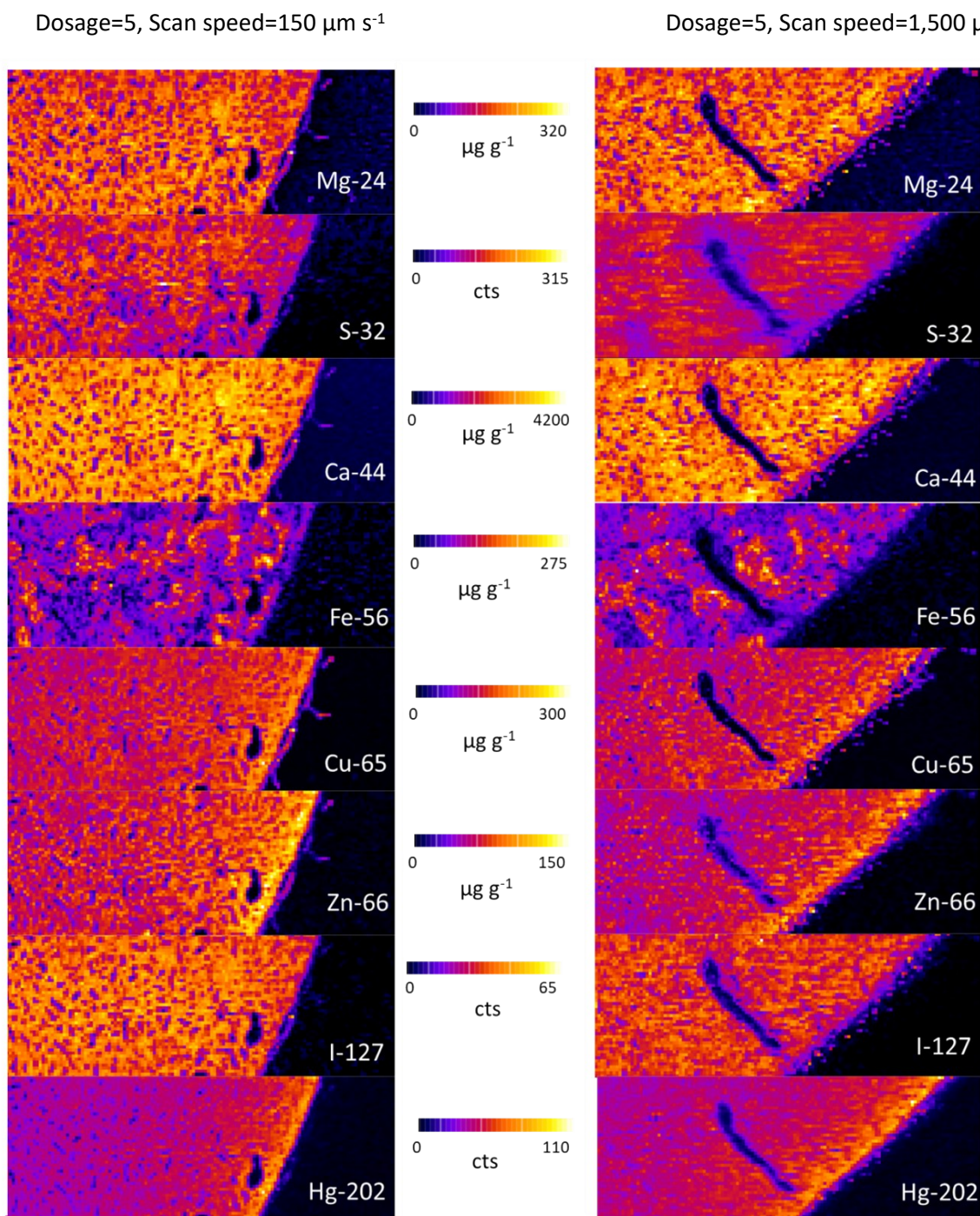


Fig S3 Element maps ($1,950 \times 750 \mu\text{m}^2$) generated by LA-ICP-TOFMS analysis of kidney tissue at a dosage of 5, comparing “slow” (left column) and “fast” (right column) mapping modes. Map intensities are reported in either $\mu\text{g g}^{-1}$ or counts, depending on the element's availability in the gelatin standard used for calibration.